

## Large-Scale Vegetation Feedbacks on a Doubled CO<sub>2</sub> Climate

SAMUEL LEVIS

*National Center for Atmospheric Research, Boulder, Colorado*

JONATHAN A. FOLEY

*Climate, People, and Environment Program, Institute for Environmental Studies, University of Wisconsin—Madison, Madison, Wisconsin*

DAVID POLLARD

*Earth System Science Center, The Pennsylvania State University, University Park, Pennsylvania*

(Manuscript received 22 February 1999, in final form 10 June 1999)

### ABSTRACT

Changes in vegetation cover are known to influence the climate system by modifying the radiative, momentum, and hydrologic balance of the land surface. To explore the interactions between terrestrial vegetation and the atmosphere for doubled atmospheric CO<sub>2</sub> concentrations, the newly developed fully coupled GENESIS-IBIS climate-vegetation model is used. The simulated climatic response to the radiative and physiological effects of elevated CO<sub>2</sub> concentrations, as well as to ensuing simulated shifts in global vegetation patterns is investigated.

The radiative effects of elevated CO<sub>2</sub> concentrations raise temperatures and intensify the hydrologic cycle on the global scale. In response, soil moisture increases in the mid- and high latitudes by 4% and 5%, respectively. Tropical soil moisture, however, decreases by 5% due to a decrease in precipitation minus evapotranspiration.

The direct, physiological response of plants to elevated CO<sub>2</sub> generally acts to weaken the earth's hydrologic cycle by lowering transpiration rates across the globe. Lowering transpiration alone would tend to enhance soil moisture. However, reduced recirculation of water in the atmosphere, which lowers precipitation, leads to more arid conditions overall (simulated global soil moisture decreases by 1%), particularly in the Tropics and mid-latitudes.

Allowing structural changes in the vegetation cover (in response to changes in climate and CO<sub>2</sub> concentrations) overrides the direct physiological effects of CO<sub>2</sub> on vegetation in many regions. For example, increased simulated forest cover in the Tropics enhances canopy evapotranspiration overall, offsetting the decreased transpiration due to lower leaf conductance. As a result of increased circulation of moisture through the hydrologic cycle, precipitation increases and soil moisture returns to the value simulated with just the radiative effects of elevated CO<sub>2</sub>. However, in the highly continental midlatitudes, changes in vegetation cover cause soil moisture to decline by an additional 2%. Here, precipitation does not respond sufficiently to increased plant-water uptake, due to a limited source of external moisture into the region.

These results illustrate that vegetation feedbacks may operate differently according to regional characteristics of the climate and vegetation cover. In particular, it is found that CO<sub>2</sub> fertilization can cause either an increase or a decrease in available soil moisture, depending on the associated changes in vegetation cover and the ability of the regional climate to recirculate water vapor. This is in direct contrast to the view that CO<sub>2</sub> fertilization will enhance soil moisture and runoff across the globe: a view that neglects changes in vegetation structure and local climatic feedbacks.

### 1. Introduction

The potential climatic and societal impacts of increased atmospheric CO<sub>2</sub> concentrations has concerned the scientific community for over a century (e.g., Arrhenius 1896). Numerous simulations performed with

global climate models (GCMs), as compiled in the 1995 Intergovernmental Panel on Climate Change report, concur that doubling the concentration of atmospheric CO<sub>2</sub> (but neglecting the impact of increasing aerosols) results in a global average warming at the earth's surface of between 1.5° and 4.5°C (Kattenberg et al. 1996). In most simulations, the warming is accompanied by an intensified global hydrologic cycle. Also, all these simulations show pronounced changes in regional climate. For example, many models show a decline in midcontinental soil moisture, due to an overall decrease in the

---

*Corresponding author address:* Dr. Samuel Levis, NCAR, P.O. Box 3000, Boulder, CO 80307-3000.  
E-mail: slevis@ucar.edu

precipitation minus evapotranspiration (e.g., Manabe and Wetherald 1986; Rind 1988; Wetherald and Manabe 1995; Gregory et al. 1997).

It has been hypothesized that CO<sub>2</sub>-induced climate changes could be modified by changes in the earth's vegetation cover. Several modeling studies have already illustrated that altered vegetation patterns, whether due to changes in climate or to human activities, may result in significant regional and possibly global climatic feedbacks. These studies include work on tropical (e.g., Lean et al. 1996; Manzi and Planton 1996; Lean and Rowntree 1997), temperate (e.g., Bonan 1995), and boreal deforestation (e.g., Bonan et al. 1992); the onset of glacial climates (e.g., de Noblet et al. 1996; Gallimore and Kutzbach 1996); the Holocene expansion of boreal forests (e.g., Foley et al. 1994); and the Holocene greening of the Sahel (e.g., Kutzbach et al. 1996; Texier et al. 1997).

Other studies of climate–vegetation interactions have focused on the physiological response of plants to increased atmospheric CO<sub>2</sub> concentrations. Laboratory and field observations have shown that increased CO<sub>2</sub> concentrations can stimulate net photosynthesis (especially in C<sub>3</sub> plants) and increase the water use efficiency (i.e., moles of CO<sub>2</sub> fixed through photosynthesis per moles of H<sub>2</sub>O lost through transpiration) of most plants. This “CO<sub>2</sub> fertilization effect” is thought to generally reduce the water vapor conductance (and transpiration through stomata) of plant canopies (e.g., Polley et al. 1993; Field et al. 1995; Curtis 1996). Climate modeling studies by Costa and Foley (1999), Sellers et al. (1996), Henderson-Sellers et al. (1995), and Pollard and Thompson (1995) have shown that lowered stomatal conductance leads to general decreases in evapotranspiration (with associated increases in sensible heat flux and runoff). These decreases in evapotranspiration (latent heating) and increases in sensible heat flux can act to weaken the hydrologic cycle overall, and raise surface temperatures slightly.

Here we consider the *combined* effects of changes in vegetation cover and canopy conductance on a CO<sub>2</sub>-warmed climate (Betts et al. 1997; Levis et al. 1999a). In particular, we use a fully coupled climate–vegetation model to examine the regional characteristics of vegetation feedbacks on the climate system. We isolate the climate sensitivity to radiative and physiological effects of elevated CO<sub>2</sub>, as well as to the altered global distribution of vegetation cover. Our purpose is to investigate how vegetation feedbacks affect climate, through changes in vegetation cover and/or changes in canopy conductance in different environments. In this way, we wish to examine, in greater spatial and temporal detail than has been previously documented (Betts et al. 1997), the impacts of vegetation feedbacks on CO<sub>2</sub>-induced climate change.

## 2. Model description and methods

Growing interest in exploring the bidirectional interactions of climate and vegetation has led modelers to

couple simple equilibrium vegetation models with GCMs (Henderson-Sellers 1993; Claussen 1994; Henderson-Sellers and McGuffie 1995; de Noblet et al. 1996; Claussen 1997; Claussen and Gayler 1997; Betts et al. 1997; Texier et al. 1997; Kubatzki and Claussen 1998; Claussen 1998; Claussen et al. 1998). The preferred coupling scheme involves a series of GCM simulations (of one to several years) interrupted by periodic updates of “equilibrium” vegetation cover within the GCM until steady-state conditions are attained. This is commonly termed *iterative coupling*.

Foley et al. (1998) recently developed a new technique for the synchronous coupling of climate and vegetation models, to overcome some of the limitations of the iterative technique. According to the synchronous scheme, coupled models should share a common description of the surface energy and water balance, in order to maintain physical consistency between joint climate and ecosystem processes. Also, by definition, synchronously coupled models should simulate transient changes in the vegetation cover, rather than discrete “equilibrium” vegetation conditions, in order to represent vegetation dynamics as an integral part of the climate system.

Foley et al. (1998) incorporated the Integrated Biosphere Simulator (IBIS) biosphere model (Foley et al. 1996) within the GENESIS GCM (version 2; Thompson and Pollard 1997). In the coupled model, GENESIS, a three-dimensional GCM, simulates the physics and general circulation of the atmosphere, while IBIS predicts transient changes in the vegetation structure. GENESIS and IBIS operate in tandem (with the same time step) around a common treatment of land surface and eco-physiological processes [based on the LSX land surface package of Pollard and Thompson (1995)] to calculate the energy, water, carbon, and momentum fluxes between vegetation, soils, and the atmosphere.

The coupled GENESIS–IBIS model was shown to simulate the basic global-scale patterns of climate and vegetation successfully. However, in a few regions, the coupled model exhibits relatively large climate biases, which result in vegetation patterns that are not consistent with observations (see Foley et al. 1998). For reference, IBIS output compares well against observations, when driven with observed climate data (Foley et al. 1996; Costa and Foley 1997).

In the present study, we employ the coupled GENESIS–IBIS model at R15 spectral horizontal resolution (~4.5° lat × 7.5° long), with 16 layers in the vertical, and a 45-min time step. This resolution allows us to perform long model integrations without great computational expense. For illustrating climate–vegetation interactions at large scales, low resolutions have proven sufficient in previous work with this model (Levis et al. 1999a,b). We have found that, while increased horizontal resolution improves the simulation regionally, on the whole it does not justify the added computational expense for exploratory investigations such as this.

### a. GENESIS: The atmosphere

The GENESIS GCM has been documented (Pollard and Thompson 1994; Pollard and Thompson 1995; Thompson and Pollard 1995a,b; Thompson and Pollard 1997; Pollard and Thompson 1997) and tested in a wide variety of climate simulations (e.g., Bonan et al. 1992; Barron et al. 1993; Crowley et al. 1993; Foley et al. 1994; Pollard et al. 1998; Foley et al. 1998) and in the Atmospheric Modelling Intercomparison Project effort (Gates 1992). In general, GENESIS version 2 (Thompson and Pollard 1997) simulates a better climate than version 1.02 (Thompson and Pollard 1995a) when compared with observations. However, both versions of the model produce a cold wintertime bias over the Himalayan plateau and China, possibly due to dynamical effects of Himalayan orography. Also, much of continental Antarctica and Greenland are warmer than observed. Zonally averaged precipitation agrees well with observations. Compared with other models of this complexity, GENESIS simulates satisfactory global climate patterns for use in the investigation of bidirectional climate–vegetation interactions.

GENESIS includes the effects of several greenhouse trace gases ( $\text{CO}_2$ ,  $\text{CH}_4$ ,  $\text{N}_2\text{O}$ , CFC11, and CFC12) explicitly, assuming globally uniform mixing ratios (Wang et al. 1991). The radiative effects of tropospheric aerosols are included, assuming a uniform aerosol column over all nonice land points, with a prescribed exponential decrease with height. In our climate change simulations, only the concentration of  $\text{CO}_2$  is doubled; other trace gas and aerosol concentrations are not changed.

In this study, sea surface temperatures are simulated using a simple thermodynamic mixed-layer representation of the upper ocean (~50 m). Sea ice is simulated using a three-layer thermodynamic model and is free to flow with prescribed ocean currents and simulated atmospheric winds.

### b. IBIS: Vegetation and the land surface

IBIS belongs to a new generation of Dynamic Global Vegetation Models (Foley et al. 1996; Friend et al. 1997; Beerling et al. 1997). IBIS in particular integrates biophysical, physiological, ecological, and hydrological processes in one model framework (Foley et al. 1996). The model's land surface package (biophysical and hydrological processes; Pollard and Thompson 1995) was evaluated against other land surface models (the PILPS effort of Henderson-Sellers et al. 1996) and against observations (Levis et al. 1996). The complete model has been evaluated at global (Foley et al. 1996) and regional (Costa and Foley 1997) scales, as well as at individual sites (Delire and Foley 1999).

Vegetation is described in IBIS as an upper and a lower canopy (trees and grasses) that captures light, intercepts water, and fixes carbon. Vegetation structure is characterized foremost by the leaf area index (LAI)

and fractional cover, but also by the amount of biomass. The structure and composition of the vegetation cover changes in response to the vegetation's annual carbon budget, and the changing competitive balance for light and soil moisture between nine plant functional types. A simple phenology model allows for the distinction between evergreen and deciduous plant types (Foley et al. 1996).

As simulated by IBIS, the physiological (i.e., photosynthesis and stomatal conductance) effects of modified atmospheric  $\text{CO}_2$  concentrations do not consider changes in whole-plant allocation or altered nutrient cycling patterns. In addition, IBIS does not account for observed nutrient availability and its consequences on plant growth. In the field under elevated  $\text{CO}_2$ , whole-plant processes and nutrient limitations are often found to reduce the  $\text{CO}_2$ -induced enhancement of productivity (Field et al. 1995).

There are six soil layers of varying thickness down to a depth of 4 m. Water may infiltrate into the soil or run off at the surface. If not frozen, soil moisture can evaporate from the top or drain out of the bottom soil layer, and it may transpire through the vegetation. Finally, snow is represented by three layers of varying thickness and fractional cover.

### c. The simulations

We consider three forcing mechanisms on the coupled climate–vegetation system: radiative effects of increased  $\text{CO}_2$  (R), physiological effects of increased  $\text{CO}_2$  (P), and changes in vegetation cover (V). For this purpose, we conduct four coupled model simulations:

- Modern climate and vegetation (control)
- Doubled  $\text{CO}_2$  climate (R)
- Doubled  $\text{CO}_2$  climate, where canopy *physiology* responds to elevated  $\text{CO}_2$  (RP)
- Doubled  $\text{CO}_2$  climate, where canopy *physiology* responds to elevated  $\text{CO}_2$  and *vegetation cover* responds to elevated  $\text{CO}_2$  and to changes in climate (RPV)

All simulations are performed for equilibrium conditions; transient changes in  $\text{CO}_2$  concentrations and their effects on climate are not considered in this study. In the control we prescribe atmospheric  $\text{CO}_2$  concentrations at 345 ppmv; in R, RP, and RPV,  $\text{CO}_2$  concentrations are set to 690 ppmv.

The Control and RPV are 70-yr simulations (starting from a previous 50-yr equilibrium simulation of the modern climate), in which the vegetation cover is allowed to roughly equilibrate with the simulated climate. Here R and RP are 20-yr simulations with prescribed vegetation cover obtained from the control.

## 3. Results

Due to our interest in land surface feedbacks, we examine model output averaged over ice-free continen-

tal regions for the last 10 years of each simulation. In presenting the model results, we follow a stepwise approach (the control, R, RP, and RPV), in order to isolate the selected forcing mechanisms (R, P, and V).

We report temperatures and fluxes from the lowest GCM level ( $\sim 50$  m above the surface). Simulated evapotranspiration includes contributions from land surfaces as well as fractional open water (lakes, wetlands, and coastal waters) in every model grid cell. Such water bodies are treated as unlimited sources of water and, therefore, do not permit the hydrologic cycle to balance exactly. Also, a model assumption in IBIS causes stomatal conductance (and, therefore, transpiration) to remain infinitesimally, yet not negligibly, above zero even when soils are dry. This leads to slightly overestimated transpiration values.

#### a. Present-day climate

We briefly evaluate the present-day hydrologic cycle and climate simulation against observations averaged globally and zonally over ice-free continental regions.

The simulated global average precipitation rate is  $2.12 \text{ mm day}^{-1}$ , which is less than the observational estimates of  $2.37 \text{ mm day}^{-1}$  (UNESCO 1978),  $2.21 \text{ mm day}^{-1}$  (Baumgartner and Reichel 1975),  $2.38 \text{ mm day}^{-1}$  (Legates and Willmott 1990), and  $2.24 \text{ mm day}^{-1}$  (Leemans and Cramer 1990; W. P. Cramer 1996, personal communication). The simulated temperature of  $14.9^\circ\text{C}$  is somewhat warmer than the observational estimates of  $13.9^\circ\text{C}$  (Legates and Willmott 1990) and  $13.3^\circ\text{C}$  (Leemans and Cramer 1990; W. P. Cramer 1996, personal communication).

The model generally reproduces the observed zonal features of these variables (Figs. 1a,b). However, runoff (Fig. 1c) appears underestimated due to a systematic overestimation in the simulated evapotranspiration. In particular, a model assumption (in IBIS) that causes stomatal conductance (and transpiration) to remain nonzero even when soils are dry, leads to slightly (on the order of 1%) overestimated evapotranspiration values.

#### b. Doubled $\text{CO}_2$ climate: Global average results

Doubling the atmospheric concentration of  $\text{CO}_2$  results in a global (land plus ocean) average  $2.5^\circ\text{C}$  warming of the surface air temperature in simulation R compared to the control. This result falls within the  $1.5^\circ\text{C}$ – $4.5^\circ\text{C}$  warming reported by IPCC 1995 as simulated by equilibrium models without aerosol cooling (Kattenberg et al. 1996). This change is accompanied by an overall intensification of the hydrologic cycle, including a  $0.11 \text{ mm day}^{-1}$  increase in both precipitation and evapotranspiration over ice-free continental regions (Table 1), in agreement with past work (Kattenberg et al. 1996). A more complete analysis of the GENESIS model's doubled- $\text{CO}_2$  sensitivity is presented by Thompson and Polard (1997).

In simulation RP, IBIS allows stomatal conductance and photosynthesis to respond to the doubled atmospheric  $\text{CO}_2$  concentration. As a result, globally averaged canopy conductance decreases by about 12% (simulation RP minus R; Table 1). Simulated canopy conductance is proportional to the net photosynthesis and inversely proportional to atmospheric  $\text{CO}_2$  concentrations. Increased  $\text{CO}_2$  concentrations cause photosynthesis rates (as measured by canopy net primary productivity, NPP) to increase by 62%, primarily due to the  $\text{CO}_2$  fertilization effect on  $\text{C}_3$  photosynthesis. This productivity increase largely offsets the decrease in canopy conductance due directly to the increase in  $\text{CO}_2$ . Overall, the decrease in canopy conductance causes a decrease in transpiration (evapotranspiration) of  $0.03 \text{ mm day}^{-1}$  ( $0.02 \text{ mm day}^{-1}$ ) on the global mean. In response, precipitation decreases by  $0.07 \text{ mm day}^{-1}$  and the temperature rises by  $0.2^\circ\text{C}$ . These results qualitatively agree with the results of Sellers et al. (1996).

Simulation RPV includes all three forcing factors: radiative forcing from increasing  $\text{CO}_2$  (R), physiological impacts of increasing  $\text{CO}_2$  (P), and the consequent changes in simulated vegetation cover (V). In RPV, the global average LAI increases from 4.3 to  $6.4 \text{ m}^2 \text{ m}^{-2}$ . This increase is associated with an expansion of forest cover at the expense of grasses, and can be explained in part by the differential impact of  $\text{CO}_2$  fertilization on  $\text{C}_3$  plant types (including all trees and cool grasses) and  $\text{C}_4$  plant types (tropical grasses) (Idso and Kimball 1993). In RPV, we find no significant additional change in temperature compared to RP. However, continental precipitation and evapotranspiration both increase by  $0.06 \text{ mm day}^{-1}$ . The increase in evapotranspiration is associated with a  $0.08 \text{ mm day}^{-1}$  rise in transpiration, which, in turn, is attributed to the  $2.1 \text{ m}^2 \text{ m}^{-2}$  increase in canopy density (i.e., LAI) across the globe. Therefore, on a global scale, changes in the vegetation cover appear to partially offset the effects of reduced canopy conductance (Table 1), in overall agreement with Betts et al. (1997).

#### c. Northern high latitudes ( $60^\circ$ – $90^\circ\text{N}$ )

##### 1) SIMULATION R MINUS CONTROL

The annual average high-latitude warming of  $3.9^\circ\text{C}$  in simulation R compared to the control (Table 2) is greatest during fall, winter, and spring (January maximum of  $\sim 7^\circ\text{C}$ ; Fig. 2a), consistent with numerous other GCM simulations (Kattenberg et al. 1996). The cold-season peak in the warming suggests the presence of positive feedbacks caused by reduced snow cover on the land and reduced sea ice on the Arctic Ocean (e.g., Dickinson et al. 1987; Harvey 1988; Curry et al. 1995; Rind et al. 1995; Kattenberg et al. 1996).

Precipitation increases throughout the year by  $0.15 \text{ mm day}^{-1}$  (Table 2) and follows a similar seasonal cycle as the temperature (Fig. 2b), illustrating 1) the direct

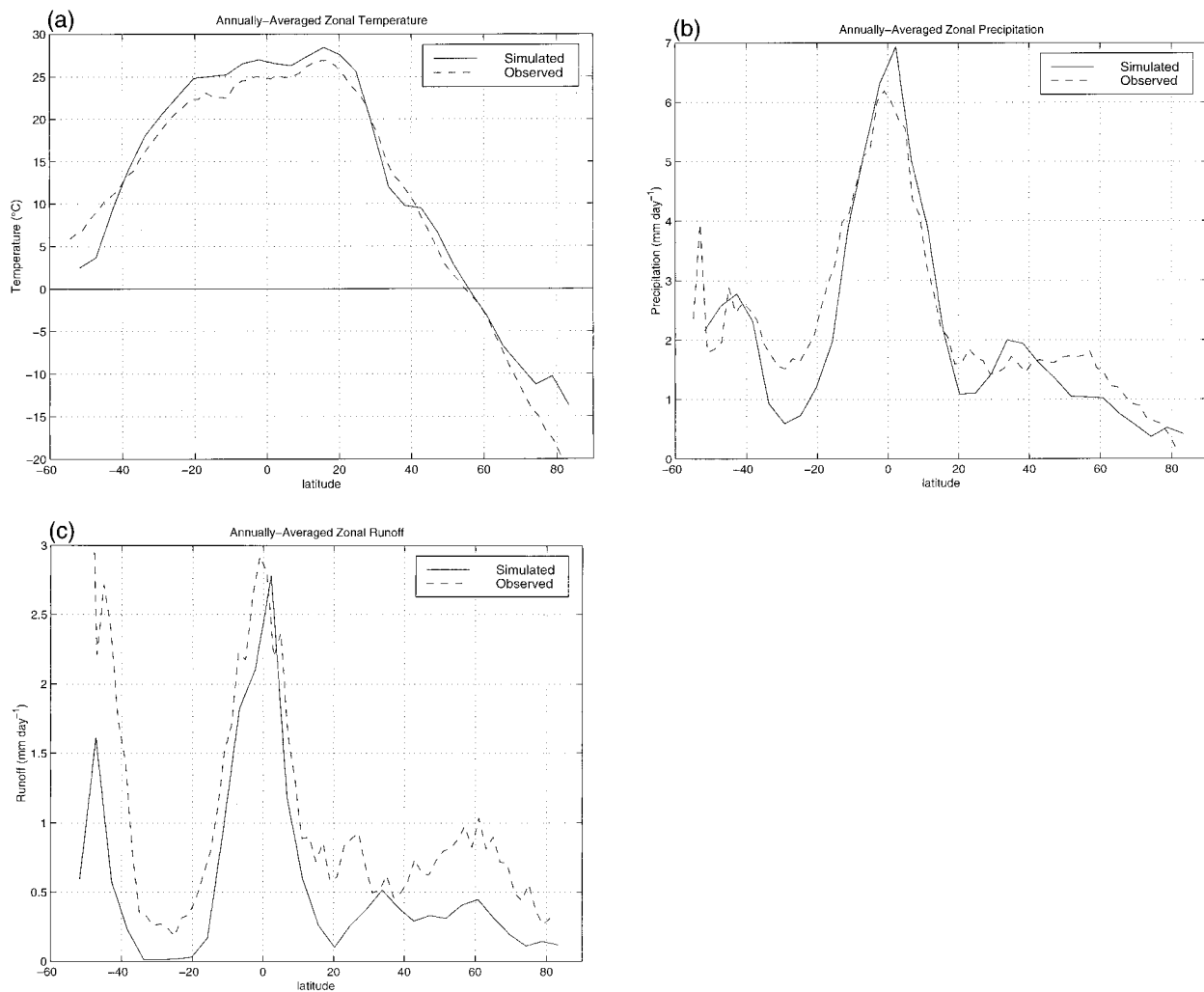


FIG. 1. Zonally averaged (a) temperature, (b) precipitation, and (c) runoff over ice-free continents (simulated vs observed). We report observed temperature and precipitation from Legates and Willmott (1990) and run off from Cogley (1991).

connection between temperature and the water holding capacity of air, and 2) an unrestricted source of water vapor (from increasingly ice-free Arctic Ocean waters and from increased moisture storage in the soils).

With the warmer and wetter conditions, evapotrans-

piration increases year-round by  $0.09 \text{ mm day}^{-1}$  (Table 2), with a peak in summer (Fig. 2c). Soil moisture increases year-round by 5% (Table 2), due to more precipitation and less frozen soils, which allow for more infiltration and percolation.

TABLE 1. Globally averaged near-surface environmental variables over ice-free continental regions for the control simulation. Also, globally averaged differences of the same variables between simulations R and the control, RP and R, and RPV and RP. For reference, we show the globally averaged (land plus ocean) temperature and its differences.

	Control	R-Control	RP-R	RPV-RP
Global temperature (°C)	14.5	+2.5	+0.1	0.0
Temperature (°C)	14.9	+2.7	+0.2	0.0
Sensible heat ( $\text{W m}^{-2}$ )	27.0	+0.8 (+3%)	+0.6 (+2%)	-1.1 (-4%)
Precipitation ( $\text{mm day}^{-1}$ )	2.12	+0.11 (+5%)	-0.07 (-3%)	+0.06 (+3%)
Evapotranspiration ( $\text{mm day}^{-1}$ )	1.75	+0.11 (+6%)	-0.02 (-1%)	+0.06 (+3%)
Transpiration ( $\text{mm day}^{-1}$ )	0.81	+0.05 (+6%)	-0.03 (-3%)	+0.08 (+10%)
Soil water (m in 4-m column)	0.85	-0.01 (-1%)	-0.01 (-1%)	0.00 (0%)
Canopy conductance ( $\text{mm s}^{-1}$ )	0.59	-0.01 (-2%)	-0.07 (-12%)	+0.13 (+25%)
Leaf area index ( $\text{m}^2 \text{ m}^{-2}$ )	4.3	Unchanged	Unchanged	+2.1

TABLE 2. As in Table 1 but averaged over ice-free continents of the northern high latitudes ( $60^{\circ}$ – $90^{\circ}$ N). We show simulated surface albedo for this region, as well as simulated sea ice cover for water bodies north of  $60^{\circ}$ N.

	Control	R–Control	RP–R	RPV–RP
Temperature ( $^{\circ}$ C)	–6.7	+3.9	+0.6	0.0
Sensible heat ( $\text{W m}^{-2}$ )	4.0	+0.5 (+13%)	0.00 (0%)	+1.3 (+29%)
Precipitation ( $\text{mm day}^{-1}$ )	0.76	+0.15 (+20%)	+0.02 (+2%)	+0.02 (+2%)
Evapotranspiration ( $\text{mm day}^{-1}$ )	0.35	+0.09 (+26%)	0.00 (0%)	+0.05 (+11%)
Transpiration ( $\text{mm day}^{-1}$ )	0.15	+0.03 (+20%)	–0.02 (–11%)	+0.11 (+69%)
Soil water (m in 4-m column)	0.99	+0.05 (+5%)	+0.02 (+2%)	+0.01 (+1%)
Canopy conductance ( $\text{mm s}^{-1}$ )	0.28	+0.02 (+7%)	–0.06 (–20%)	+0.18 (+75%)
Leaf area index ( $\text{m}^2 \text{m}^{-2}$ )	2.5	Unchanged	Unchanged	+3.0
Surface albedo (fraction)	0.38	–0.03	0.00	–0.06
Sea ice cover (fraction)	0.48	–0.11	–0.02	+0.01

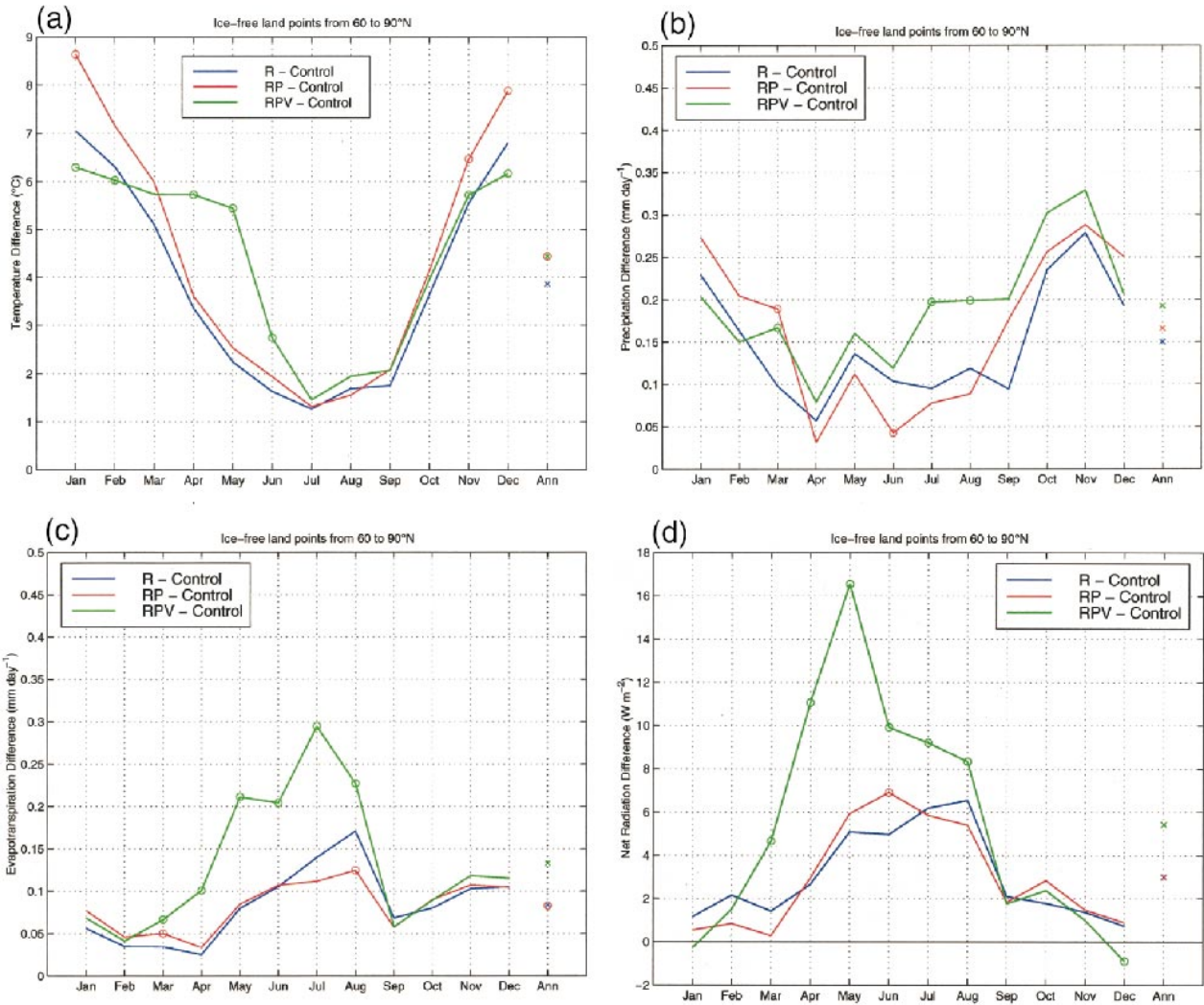


FIG. 2. Ice-free continental regions of the northern high latitudes ( $60^{\circ}$ – $90^{\circ}$ N). Monthly average differences in simulated (a) temperature, (b) precipitation, (c) evapotranspiration, and (d) net radiation. *Blue line*: changes due to  $\text{CO}_2$  radiative forcing (R – control); *red line*: changes due to  $\text{CO}_2$  radiative and physiological forcing (RP – control); *green line*: changes due to  $\text{CO}_2$  radiative and physiological forcing with vegetation feedbacks (RPV – control). Statistically significant changes of RP – R and RPV – RP (at the 95% confidence level, using a Student's t-test) are shown with open circles. Here R – control is always significant; therefore, circles are omitted. We report temperature and fluxes from the lowest GCM level ( $\sim 50$  m above the surface).

TABLE 3. As in Table 2 but averaged over midlatitude continents (30°–60°N).

	Control	R-Control	RP-R	RPV-RP
Temperature (°C)	6.9	+2.7	+0.3	0.0
Sensible heat ( $W m^{-2}$ )	22.6	-0.9 (-4%)	+1.1 (+5%)	-1.1 (-5%)
Precipitation ( $mm day^{-1}$ )	1.51	+0.19 (+13%)	-0.07 (-4%)	+0.05 (+3%)
Evapotranspiration ( $mm day^{-1}$ )	1.16	+0.14 (+12%)	-0.03 (-2%)	+0.07 (+6%)
Transpiration ( $mm day^{-1}$ )	0.55	+0.07 (+13%)	-0.03 (-5%)	+0.11 (+19%)
Soil water (m in 4-m column)	0.84	+0.03 (+4%)	-0.01 (-1%)	-0.02 (-2%)
Canopy conductance ( $mm s^{-1}$ )	0.57	+0.03 (+5%)	-0.09 (-15%)	+0.18 (+37%)
Leaf area index ( $m^2 m^{-2}$ )	5.0	Unchanged	Unchanged	+2.4
Surface albedo (fraction)	0.17	-0.01	0.00	-0.01

## 2) SIMULATION RP MINUS R

In simulation RP compared to R, we find an additional high-latitude warming of 0.6°C (Table 2 and Fig. 2a) due to a decrease in evapotranspiration in late summer (Fig. 2c) and the resultant positive feedback of diminishing sea ice on the Arctic Ocean. This oceanic feedback explains the seasonality in the warming of this region, as described for simulation R.

Annual-average transpiration decreases in RP by 0.02  $mm day^{-1}$  with a peak in summer, that is, during the growing season, in direct response to the physiological effects of elevated  $CO_2$  on leaf stomata (Table 2). Evapotranspiration (Fig. 2c) does not change appreciably, because increases in evaporation from the ground and canopy (not shown) compensate for the decrease in transpiration. This implies ample water availability, which can be attributed to the 0.02  $mm day^{-1}$  annual increase in precipitation (Fig. 2b) and the 2% increase in soil moisture (Table 2).

The physiological effects of elevated  $CO_2$  on high-latitude temperature and precipitation appear similar to (and generally amplify) the radiative feedbacks (R minus Control), leading to progressively warmer and wetter conditions.

## 3) SIMULATION RPV MINUS RP

In simulation RPV, the vegetation cover responds to the extension of the growing season in the high latitudes, in addition to the physiological effects of doubled  $CO_2$  concentrations. As a result, the LAI increases greatly, from 2.5  $m^2 m^{-2}$  (in control) to 5.5  $m^2 m^{-2}$  (in RPV; Table 2), in qualitative agreement with previous projections of increased high-latitude forest density and extent (Prentice et al. 1991; Neilson and Marks 1994; Starfield and Chapin 1996).

The climate-induced changes in vegetation cover enhance the high-latitude continental warming by 1.6°C and 0.5°C in spring and summer, respectively (Fig. 2a). This positive feedback results from the decrease in surface albedo (Table 2) between expanded boreal forests and retreating snow-covered tundra regions (Laine and Heikinheimo 1996; Robinson and Kukla 1985; Sharratt 1998). The same process has been shown to apply in simulations of the warmer mid-Holocene (Foley et al.

1994; Ganopolski et al. 1998) as well as, in reverse, under boreal deforestation conditions (e.g., Bonan et al. 1992).

Conversely, the changes in vegetation cover appear to cool the high latitudes in fall and winter by 0.3°C and 1.7°C, respectively (relative to RP; Figure 2a). This negative feedback is attributed to greater surface emissivity and, therefore, greater heat loss by terrestrial radiation (net solar minus terrestrial shown in Fig. 2d) in regions with increased forest canopy cover (Kurvonen et al. 1998). In fall and winter, the changes in surface albedo have little effect on this region's energy balance, because insolation drops to a minimum. The cooling extends into the lower atmosphere, in part because of a slight decrease in the negative sensible heat flux as a direct result of the greater surface roughness in regions of denser vegetation (Bonan et al. 1995; Levis et al. 1999a) (note: sensible heat is usually negative during high-latitude winters). The infrared heat loss (and cooling) is amplified by enhanced atmospheric stability in the region (enhanced subsidence), which results in decreased cloudiness (not shown). Further observational evidence may help verify the potential for this negative feedback mechanism on high-latitude greenhouse warming.

The warming feedback in spring and summer is accompanied by an increase in precipitation (Fig. 2b), evapotranspiration (Fig. 2c), and snowmelt. The cooling in winter is accompanied by a decrease in the precipitation. These results emphasize the importance of the relationship between temperature and the water holding capacity of air in the high latitudes. Finally, soil moisture increases year-round, because warmer spring and summer temperatures facilitate water infiltration into less frozen soils (Table 2).

## d. Northern midlatitudes (30°–60°N)

### 1) SIMULATION R MINUS CONTROL

In the midlatitudes, the radiative warming (R minus the control) is weaker (2.7°C; Table 3) and has a narrower seasonal range than in the high latitudes (Fig. 3a). This is partly due to a smaller change in snow and sea ice cover between simulations R and the control in this region.

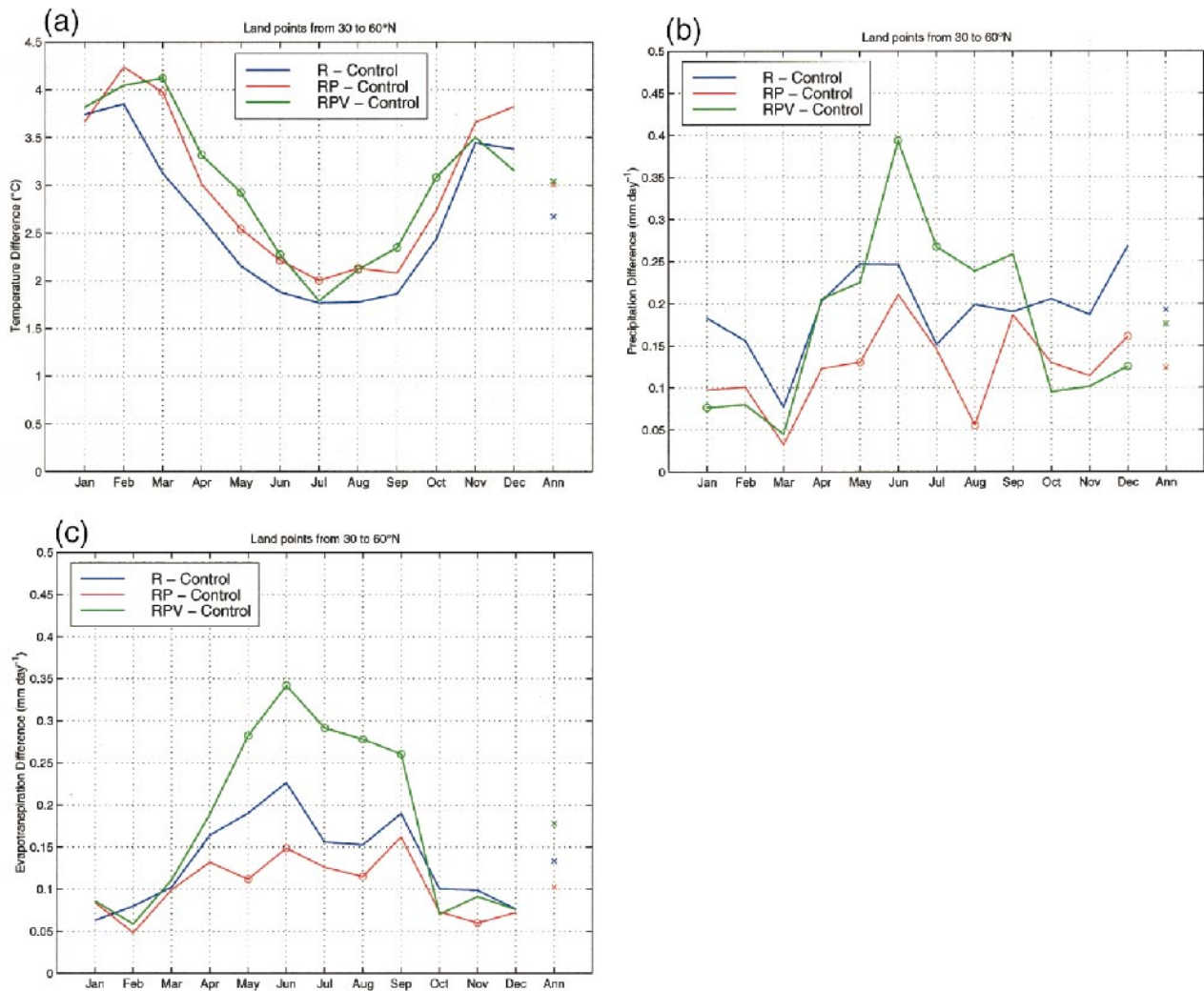


FIG. 3. As in Figs. 2a–c but for continental regions of the midlatitudes (30°–60°N). For better resolution, the temperature scale is half that in Fig. 2.

Precipitation (Fig. 3b) and evapotranspiration (Fig. 3c) increase year round by  $0.19 \text{ mm day}^{-1}$  and  $0.14 \text{ mm day}^{-1}$ , respectively, leading to increases in the soil moisture (4%; Table 3). As in the high latitudes, the hydrologic cycle intensifies in response to the greater water holding capacity of warmer air and the large increase of oceanic evaporation rates. However, zonal-average changes in the hydrologic cycle mask the significant drying that appears in large parts of continental Asia (not shown), in qualitative agreement with much of the climate change literature discussing midcontinental aridity as an effect of global warming (e.g., Manabe and Wetherald 1986; Rind 1988; Wetherald and Manabe 1995; Gregory et al. 1997).

## 2) SIMULATION RP MINUS R

The physiological effects of doubled  $\text{CO}_2$  concentrations generate an additional year-round warming in the

midlatitudes (on average  $0.3^\circ\text{C}$ , relative to R) in response to a  $0.03 \text{ mm day}^{-1}$  reduction in evapotranspiration. Precipitation decreases by  $0.07 \text{ mm day}^{-1}$  and soil moisture by 1% year-round (Table 3 and Fig. 3).

The physiological impacts of doubled  $\text{CO}_2$  influence the hydrologic cycle of this region in two ways, with opposite effects on the soil moisture: 1) transpiration is reduced by improved plant water-use efficiency, but, as a result 2) less water is recycled through the atmosphere for precipitation. Ultimately, soil moisture is depleted, because the second mechanism prevails. A positive soil moisture feedback (see Eltahir 1998) potentially contributes to the drier water balance, by reducing moist static energy in the boundary layer and inhibiting precipitation.

Midlatitude climate shows stronger direct sensitivity to changes in plant transpiration than high-latitude climates. This is partly due to the longer growing season in the midlatitudes, which, through photosynthesis,

makes transpiration a more significant component of the hydrologic cycle. In addition, greater overall continentality increases the sensitivity of the hydrologic cycle to local recirculation of soil moisture. Therefore, a larger fraction of the precipitation in this region relies on the recycling of water through evapotranspiration (Delworth and Manabe 1989).

### 3) SIMULATION RPV MINUS RP

In simulation RPV, where the structure of the vegetation cover responds to changes in climate and CO<sub>2</sub> concentrations, LAI values increase throughout the midlatitudes, including in semi-arid regions (LAI increases from 5.0 to 7.4 m<sup>2</sup> m<sup>-2</sup> on average; Table 3). We find increases in the LAI primarily of temperate deciduous trees (United States and western Europe) and of midcontinental grasses (Eurasia). Evergreen tree LAIs increase in East Asia and in limited parts of the United States.

Midlatitude spring and fall are slightly warmer in RPV than in RP (Fig. 3a), in response to the increase in vegetation cover and the resultant decrease in the surface albedo. In December, there is a slight, yet regionally statistically significant cooling, due to increased emissivity of denser vegetation (as shown for the high latitudes). Finally in July, there is a small, yet regionally statistically significant cooling, due to the increase in LAI and the enhanced evapotranspiration rates (Table 3), which result in increased latent (at the expense of sensible) heat flux into the atmosphere.

The significant increase in evapotranspiration throughout the growing season (annually 0.07 mm day<sup>-1</sup>) results in spring and summer increases in the precipitation (Fig. 3b). Although precipitation increases by 0.05 mm day<sup>-1</sup> annually, soil moisture decreases by 2%, due to the increased water uptake by plants (Table 3). This response reinforces the hypothesis that a large fraction of the precipitation in this region depends on local recycling of the water reserves through evapotranspiration (Delworth and Manabe 1989).

#### e. Tropics (15°S–15°N)

##### 1) SIMULATION R MINUS CONTROL

There is a simulated 2.1°C warming in the continental Tropics (Fig. 4a), due to the radiative effects of elevated CO<sub>2</sub>. Precipitation increases in the intertropical convergence zone (ITCZ) and decreases elsewhere (annual average increase of 0.12 mm day<sup>-1</sup>). Evapotranspiration increases everywhere by 0.17 mm day<sup>-1</sup>, primarily due to the warming. Soil moisture increases in the ITCZ but on average decreases in the Tropics by 5% (Table 4).

##### 2) SIMULATION RP MINUS R

There is an additional slight warming of 0.1°C in the Tropics due to the physiological effects of elevated CO<sub>2</sub>.

Precipitation and soil moisture decrease year-round by 0.17 mm day<sup>-1</sup> and 2%, respectively (Fig. 4b and Table 4). Evapotranspiration and transpiration do not change appreciably, despite improved plant water-use efficiency, due to the offsetting effect of CO<sub>2</sub> fertilization on plant productivity.

As in the midlatitudes, the physiological feedback of narrower stomatal openings opposes the radiative effects of elevated CO<sub>2</sub> on the hydrologic cycle, in agreement with Costa and Foley (1999). In particular, the decrease in precipitation is linked partly to a small decrease in evapotranspiration and partly to a positive soil moisture feedback mechanism, by which drier soils and reduced evapotranspiration decrease the moist static energy of the boundary layer and, thus, inhibit precipitation (Eltahir 1998).

### 3) SIMULATION RPV MINUS RP

In RPV, LAI values increase throughout the Tropics. Both evergreen and deciduous trees increase their productivity (average tree LAIs change from 4.5 to 6.9 m<sup>2</sup> m<sup>-2</sup>), at the expense of tropical grasses (herbaceous LAIs change from 0.7 to 0.5 m<sup>2</sup> m<sup>-2</sup>; Table 4). The large increase in plant biomass (respiring tissue) causes NPP to decline slightly relative to simulation RP.

The changes in vegetation cover appear to nullify the physiological feedbacks shown in RP. In particular, evapotranspiration increases by 0.17 mm day<sup>-1</sup> (compared to RP), which contributes to year-round cooling of 0.1°C, as well as to increases in the precipitation (0.20 mm day<sup>-1</sup>) and soil moisture (2%; Table 4 and Fig. 4). In contrast to the midlatitudes, the tropical hydrologic cycle is enhanced without further depletion of the soil water reserves.

## 4. Conclusions

We use a fully coupled model of climate and vegetation to examine how the climate system responds to three forcing mechanisms: radiative effects of elevated CO<sub>2</sub>, physiological effects of elevated CO<sub>2</sub>, and the ensuing changes in vegetation cover. The simulated climatic response to the radiative effects of elevated CO<sub>2</sub> is in general agreement with previous simulations of its kind.

In our model, plant photosynthesis and conductance respond nonlinearly to rising CO<sub>2</sub> concentrations leading, in general, to increases in vegetation canopy density and extent on the land surface. Increased vegetation cover is shown to enhance evapotranspiration and strengthen the hydrologic cycle, while decreased canopy conductance weakens it. The net effect of the two opposing processes depends on regional moisture availability, the fraction of precipitation that originates from local recycling, and the sensitivity of the atmosphere to changes in the hydrologic cycle.

In tropical regions, the atmosphere and soils provide

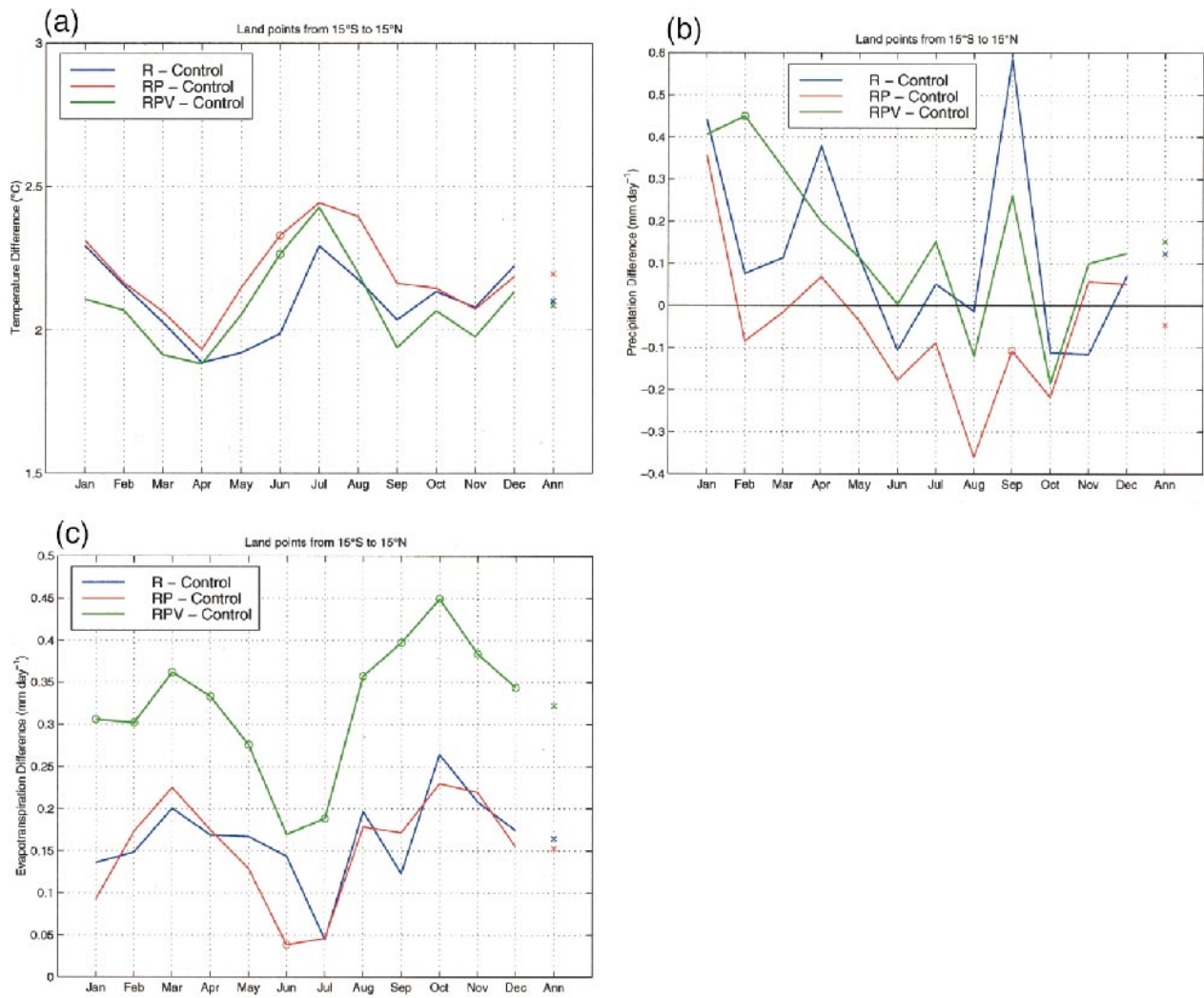


FIG. 4. As in Figs. 3a–c but for continental regions of the Tropics (15°S–15°N). For better resolution, the temperature scale is one-third that in Fig. 3. The precipitation scale is double that in Fig. 3.

copious amounts of moisture. Also, from an atmospheric dynamics perspective, the region is known for a highly unstable troposphere with a propensity for large-scale convection. As a result, increased vegetation cover enhances transpiration more than decreased stomatal conductance weakens it and triggers a positive feedback throughout the hydrologic cycle, which leads to increased precipitation and wetter soils.

In the highly continental midlatitudes, much of the precipitation originates from local recirculation of soil moisture. In addition, the midlatitude troposphere is characterized by comparatively stable conditions, especially over midcontinental regions. Therefore, the limited supply of moisture in the atmosphere and soils is accelerated through the hydrologic cycle by the increased plant-water uptake, and soil moisture and run

TABLE 4. As in Table 3 but averaged over tropical continents (15°S–15°N).

	Control	R–Control	RP–R	RPV–RP
Temperature (°C)	26.6	+2.1	+0.1	–0.1
Sensible heat ( $\text{W m}^{-2}$ )	30.7	+2.8 (+9%)	+1.0 (+3%)	–5.2 (–15%)
Precipitation ( $\text{mm day}^{-1}$ )	5.22	+0.12 (+2%)	–0.17 (–3%)	+0.20 (+4%)
Evapotranspiration ( $\text{mm day}^{-1}$ )	3.50	+0.17 (+5%)	–0.02 (–1%)	+0.17 (+5%)
Transpiration ( $\text{mm day}^{-1}$ )	1.92	+0.06 (+3%)	–0.02 (–1%)	+0.15 (+8%)
Soil water (m in 4-m column)	1.29	–0.07 (–5%)	–0.03 (–2%)	+0.02 (+2%)
Canopy conductance ( $\text{mm s}^{-1}$ )	1.04	–0.06 (–6%)	–0.09 (–9%)	+0.24 (+27%)
Leaf area index ( $\text{m}^2 \text{m}^{-2}$ )	5.2	Unchanged	Unchanged	+2.2

off (not shown) are reduced. In other words, evapotranspiration increases more than precipitation.

In this study, we have made significant progress in capturing a wide range of interacting nonlinear processes within the climate system. Our intention is to improve our understanding of the Earth System and its potential responses to anthropogenic environmental change. On one hand, our model results agree with projections for a “greener” Earth through CO<sub>2</sub> fertilization effects and improved plant water-use efficiency (e.g., Drake et al. 1997; Idso and Idso 1994; Graybill and Idso 1993). From water budget considerations, however, our results do not appear as optimistic as Idso and Brazel (1984) or Aston (1984), who suggest that plant physiological responses to elevated CO<sub>2</sub> will conserve water and increase stream flow in certain parts of the world.

Despite this progress, our model has room for development:

- The physiological effects of increasing CO<sub>2</sub> concentrations simulated here do not consider changes in whole-plant allocation or nutrient cycling patterns, which may act to reduce the CO<sub>2</sub>-induced enhancement of productivity (Field et al. 1995). Therefore, the “greening” (in simulation RPV of this study) may be considered a high estimate of the biosphere’s response to doubled CO<sub>2</sub>.
- Milly (1997) has shown that continental aridity may depend in part on plant rooting characteristics. GENESIS-IBIS does not simulate explicitly the response of plant-water uptake to changes in below ground biomass (i.e., root volume).
- GENESIS-IBIS does not account for changes in natural disturbances, such as fires. Warmer and drier conditions in certain parts of the world may increase the frequency of fires (Overpeck et al. 1990; Ryan 1991), thereby curbing the potential biospheric enhancement under elevated CO<sub>2</sub>.
- To examine the potential climatic feedback mechanisms presented in this study at finer scales (e.g., for the application in climate change policy) we need to operate fully coupled ocean-atmosphere-biosphere models. With a synchronously coupled model, such as GENESIS-IBIS, we may begin to simulate processes of climate-vegetation change due to transient trends in CO<sub>2</sub>. Here, the model is not coupled to a dynamic ocean model.
- We must begin to examine the effects of human land use as another interactive component of the climate system.

*Acknowledgments.* The authors would like to thank C. Molling and R. Doherty for technical assistance with the simulations and data processing. Comments from M. Coe and two anonymous reviewers substantially improved the manuscript. This work was supported by NSF Grant ATM-9711484 and NASA Grant NAG5-3513. The computer simulations were, in part, con-

ducted at the NCAR Climate Simulation Laboratory Computing Grant 93300185. The National Center for Atmospheric Research (NCAR) is sponsored by the National Science Foundation (NSF).

#### REFERENCES

- Arrhenius, S., 1896: On the influence of carbonic acid in the air upon the temperature of the ground. *Philos. Mag.*, **41**, 237–276.
- Aston, A. R., 1984: Effect of doubling atmospheric CO<sub>2</sub> on streamflow: A simulation. *J. Hydrol.*, **67**, 273–280.
- Barron, E. J., W. W. Peterson, D. Pollard, and S. L. Thompson, 1993: Past climate and the role of ocean heat transport: Model simulations for the Cretaceous. *Paleoceanography*, **8**, 785–798.
- Baumgartner, A., and E. Reichel, 1975: *The World Water Balance: Mean Annual Global Continental and Maritime Precipitation, Evaporation, and Runoff*. Elsevier, 179 pp.
- Beerling, D. J., F. I. Woodward, M. Lomas, and A. J. Jenkins, 1997: Testing the responses of a dynamic global vegetation model to environmental change: A comparison of observations and predictions. *Global Ecol. Biogeogr. Letts.*, **6**, 439–450.
- Betts, R. A., P. M. Cox, S. E. Lee, and F. I. Woodward, 1997: Contrasting physiological and structural vegetation feedbacks in climate change simulations. *Nature*, **387**, 796–799.
- Bonan, G. B., 1995: Effects of land use on the climate of the United States. *Climatic Change*, **37**, 449–486.
- , D. Pollard, and S. L. Thompson, 1992: Effects of boreal forest vegetation on global climate. *Nature*, **359**, 716–718.
- , F. S. Chapin, and S. L. Thompson, 1995: Boreal forest and tundra ecosystems as components of the climate system. *Climatic Change*, **29**, 145–167.
- Claussen, M., 1994: Coupling global biome models with climate models. *Climate Res.*, **4**, 203–221.
- , 1997: Modeling bio-geophysical feedback in the African and Indian monsoon region. *Climate Dyn.*, **13**, 247–257.
- , 1998: On multiple solutions of the atmosphere-vegetation system in present-day climate. *Global Change Biol.*, **4**, 549–559.
- , and V. Gayler, 1997: The greening of the Sahara during the mid-Holocene: Results of an interactive atmosphere-biome model. *Global Ecol. Biogeogr. Letts.*, **6**, 369–377.
- , V. Brovkin, A. Ganopolski, C. Kubatzki, and V. Petoukhov, 1998: Modelling global terrestrial vegetation-climate interaction. *Philos. Trans. Roy. Soc. London B*, **353**, 53–63.
- Cogley, J. G., 1991: GGHYDRO—Global hydrological data release 2.0. Trent Climate Note 91-1, Trent University, Dept. of Geography, Peterborough, Ontario, Canada, 13 pp. [Available from Dept. of Geography, Trent University, Peterborough, ON K9J 7B8, Canada.]
- Costa, M. H., and J. A. Foley, 1997: Water balance of the Amazon Basin: Dependence on vegetation cover and canopy conductance. *J. Geophys. Res.*, **102** (D20), 23 973–23 989.
- , and —, 1999: Combined effects of deforestation and doubled atmospheric CO<sub>2</sub> concentrations on the climate of Amazonia. *J. Climate*, **13**, 18–34.
- Crowley, T. J., S. K. Baum, and K. Y. Kim, 1993: General circulation model experiments with pole-centered supercontinents. *J. Geophys. Res.*, **98**, 8793–8800.
- Curry, J. A., J. L. Schramm, and E. E. Ebert, 1995: Sea ice-albedo climate feedback mechanism. *J. Climate*, **8**, 240–247.
- Curtis, P. S., 1996: A meta-analysis of leaf gas exchange and nitrogen in trees grown under elevated carbon dioxide. *Plant, Cell Environ.*, **19**, 127–137.
- Delire, C. L., and J. A. Foley, 1999: Evaluating the performance of a land surface/ecosystem model with biophysical measurements from contrasting environments. *J. Geophys. Res.*, **104**, 16 895–16 909.
- Delworth, T., and S. Manabe, 1989: The influence of soil wetness on near-surface atmospheric variability. *J. Climate*, **2**, 1447–1462.
- de Noblet, N. I., I. C. Prentice, S. Joussaume, D. Texier, A. Botta,

- and A. Haxeltine, 1996: Possible role of atmosphere–biosphere interactions in triggering the last glaciation. *Geophys. Res. Lett.*, **23**, 3191–3194.
- Dickinson, R. E., G. A. Meehl, and W. M. Washington, 1987: Ice-albedo feedback in a CO<sub>2</sub>-doubling simulation. *Climatic Change*, **10**, 241–248.
- Drake, B. G., M. A. Gonzalez-Meler, and S. P. Long, 1997: More efficient plants: A consequence of rising atmospheric CO<sub>2</sub>? *Annu. Rev. Plant Physiol. Plant Mol. Biol.*, **48**, 609–639.
- Eltahir, E. A. B., 1998: A soil moisture rainfall feedback mechanism 1. Theory and observations. *Water Resour. Res.*, **34**, 765–776.
- Field, C. B., R. B. Jackson, and H. A. Mooney, 1995: Stomatal responses to increased CO<sub>2</sub>: Implications from the plant to the global scale. *Plant, Cell Environ.*, **18**, 1214–1225.
- Foley, J. A., J. E. Kutzbach, M. T. Coe, and S. Levis, 1994: Feedbacks between climate and boreal forests during the Holocene epoch. *Nature*, **371**, 52–54.
- , C. I. Prentice, N. Ramankutty, S. Levis, D. Pollard, S. Sitch, and A. Haxeltine, 1996: An integrated biosphere model of land surface processes, terrestrial carbon balance, and vegetation dynamics. *Global Biogeochem. Cycles*, **10**, 603–628.
- , S. Levis, I. C. Prentice, D. Pollard, and S. L. Thompson, 1998: Coupling dynamic models of climate and vegetation. *Global Change Biol.*, **4**, 561–579.
- Friend, A. D., A. K. Stevens, R. G. Knox, and M. G. R. Cannell, 1997: A process-based, terrestrial biosphere model of ecosystem dynamics (Hybrid v3.0). *Ecol. Model.*, **95**, 249–287.
- Gallimore, R. G., and J. E. Kutzbach, 1996: Role of orbitally induced changes in tundra area in the onset of glaciation. *Nature*, **381**, 503–505.
- Ganopolski, A., C. Kubatzki, M. Claussen, V. Brovkin, and V. Petoukhov, 1998: The influence of vegetation–atmosphere–ocean interaction on climate during the mid-Holocene. *Science*, **280**, 1916–1919.
- Gates, W. L., 1992: AMIP: The atmospheric model intercomparison project. *Bull. Amer. Meteor. Soc.*, **73**, 1962–1970.
- Graybill, D. A., and S. B. Idso, 1993: Detecting the aerial fertilization effect of atmospheric CO<sub>2</sub> enrichment in tree-ring chronologies. *Global Biogeochem. Cycles*, **7**, 81–95.
- Gregory, J. M., J. F. B. Mitchell, and A. J. Brady, 1997: Summer drought in northern midlatitudes in a time-dependent CO<sub>2</sub> climate experiment. *J. Climate*, **10**, 662–686.
- Harvey, L. D. D., 1988: On the role of high-latitude ice, snow, and vegetation feedbacks in the climate response to external forcing changes. *Climatic Change*, **13**, 191–224.
- Henderson-Sellers, A., 1993: Continental vegetation as a dynamic component of a global climate model: A preliminary assessment. *Climatic Change*, **23**, 337–377.
- , and K. McGuffie, 1995: Global climate models and “dynamic” vegetation changes. *Global Change Biol.*, **1**, 63–75.
- , —, and C. Gross, 1995: Sensitivity of global climate model simulations to increased stomatal resistance and CO<sub>2</sub> increases. *J. Climate*, **8**, 1738–1756.
- , —, and A. J. Pitman, 1996: The project for intercomparison of land–surface parameterization schemes (PILPS): 1992 to 1995. *Climate Dyn.*, **12**, 849–859.
- Idso, K. E., and S. B. Idso, 1994: Plant responses to atmospheric CO<sub>2</sub> enrichment in the face of environmental constraints: A review of the past 10 years’ research. *Agric. Forest Meteorol.*, **69**, 153–203.
- Idso, S. B., and A. J. Brazel, 1984: Rising atmospheric carbon dioxide concentrations may increase streamflow. *Nature*, **312**, 51–53.
- , and B. A. Kimball, 1993: Tree growth in carbon dioxide enriched air and its implications for global carbon cycling and maximum levels of atmospheric CO<sub>2</sub>. *Global Biogeochem. Cycles*, **7**, 537–555.
- Kattenberg, A., and Coauthors, 1996: Climate models—Projections of future climate. *IPCC Climate Change 1995*, R. T. Watson et al., Eds., Vol. 1, Cambridge University Press, 285–357.
- Kubatzki, C., and M. Claussen, 1998: Simulation of the global biogeophysical interactions during the last glacial maximum. *Climate Dyn.*, **14**, 461–471.
- Kurvonen, L., J. Pulliainen, and M. Hallikainen, 1998: Monitoring of boreal forests with multitemporal special microwave imager data. *Radio Sci.*, **33**, 731–744.
- Kutzbach, J. E., G. Bonan, J. Foley, and S. P. Harrison, 1996: Vegetation and soil feedbacks on the response of the African monsoon to orbital forcing in the early to middle Holocene. *Nature*, **384**, 623–626.
- Laine, V., and M. Heikinheimo, 1996: Estimation of surface albedo from NOAA AVHRR data in high latitudes. *Tellus*, **48A**, 424–441.
- Lean, J., and P. R. Rowntree, 1997: Understanding the sensitivity of a GCM simulation of Amazonian deforestation to the specification of vegetation and soil characteristics. *J. Climate*, **10**, 1216–1235.
- , C. B. Bunton, C. A. Nobre, and P. R. Rowntree, 1996: The simulated impact of Amazonian deforestation on climate using measured ABRACOS vegetation characteristics. *Amazonian Deforestation and Climate*, J. H. C. Gash et al., Eds., John Wiley and Sons, 549–576.
- Leemans, R., and W. P. Cramer, 1990: The IIASA database for mean monthly values of temperature, precipitation and cloudiness on a global terrestrial grid. IIASA Working Paper WP-90-41, International Institute for Application System Analysis, Laxenburg, Austria, 62 pp. [Available from International Institute for Applied Systems Analysis, Schlossplatz 1, A-2361 Laxenburg, Austria.]
- Legates, D. R., and C. J. Willmott, 1990: Mean seasonal and spatial variability in gauge-corrected, global precipitation. *Int. J. Climatol.*, **10**, 111–127.
- Levis, S., M. T. Coe, and J. A. Foley, 1996: Hydrologic budget of a land surface model: A global application. *J. Geophys. Res.*, **101** (D12), 16 921–16 930.
- , J. A. Foley, and D. Pollard, 1999a: Potential high-latitude vegetation feedbacks on CO<sub>2</sub>-induced climate change. *Geophys. Res. Lett.*, **26**, 747–750.
- , —, V. Brovkin, and D. Pollard, 1999b: On the stability of the high-latitude climate–vegetation system in a coupled atmosphere–biosphere model. *Global Ecol. Biogeogr. Letts.*, in press.
- Manabe, S., and R. T. Wetherald, 1986: Reduction in summer soil wetness induced by an increase in atmospheric carbon dioxide. *Science*, **232**, 626–628.
- Manzi, O., and S. Planton, 1996: Calibration of a GCM using ABRACOS and ARME data and simulation of Amazonian deforestation. *Amazonian Deforestation and Climate*, J. H. C. Gash et al., Eds., John Wiley and Sons, 505–530.
- Milly, P. C. D., 1997: Sensitivity of greenhouse summer dryness to changes in plant rooting characteristics. *Geophys. Res. Lett.*, **24**, 269–271.
- Neilson, R. P., and D. Marks, 1994: A global perspective of regional vegetation and hydrologic sensitivities from climatic-change. *J. Vegetation Sci.*, **5**, 715–730.
- Overpeck, J. T., D. Rind, and R. Goldberg, 1990: Climate-induced changes in forest disturbance and vegetation. *Nature*, **343**, 51–53.
- Pollard, D., and S. L. Thompson, 1994: Sea–ice dynamics and CO<sub>2</sub> sensitivity in a global climate model. *Atmos.–Ocean*, **32**, 449–467.
- , and —, 1995: The effect of doubling stomatal resistance in a global climate model. *Global Planet. Change*, **10**, 129–161.
- , and —, 1997: Climate and ice-sheet mass balance at the last glacial maximum from the GENESIS version 2 global climate model. *Quat. Sci. Rev.*, **16**, 841–863.
- , J. C. Bergengren, L. M. Stillwell-Soller, B. Felzer, and S. L. Thompson, 1998: Climate simulations for 10 000 and 6000 years BP using the GENESIS global climate model. *Paleoclimates*, **2**, 183–218.
- Polley, H. W., H. B. Johnson, B. D. Marino, and H. S. Mayeux, 1993:

- Increase in C3 plant water-use efficiency and biomass over Glacial to present CO<sub>2</sub> concentrations. *Nature*, **361**, 61–64.
- Prentice, I. C., M. T. Sykes, and W. Cramer, 1991: The possible dynamic response of northern forests to global warming. *Global Ecol. Biogeogr. Letts.*, **1**, 129–135.
- Rind, D., 1988: The doubled CO<sub>2</sub> climate and the sensitivity of the modeled hydrologic cycle. *J. Geophys. Res.*, **93** (D5), 5385–5412.
- , R. Healy, C. Parkinson, and D. Martinson, 1995: The role of sea ice in 2 × CO<sub>2</sub> climate model sensitivity. Part I: The total influence of sea ice thickness and extent. *J. Climate*, **8**, 449–463.
- Robinson, D. A., and G. Kukla, 1985: Maximum surface albedo of seasonally snow-covered lands in the Northern Hemisphere. *J. Climate Appl. Meteor.*, **24**, 402–411.
- Ryan, K. C., 1991: Vegetation and wildland fire: Implications of global climate change. *Environ. Int.*, **17**, 169–178.
- Sellers, P. J., and Coauthors, 1996: Comparison of radiative and physiological effects of atmospheric CO<sub>2</sub> on climate. *Science*, **271**, 1402–1406.
- Sharratt, B. S., 1998: Radiative exchange, near-surface temperature and soil water of forest and cropland in interior Alaska. *Agric. Forest Meteor.*, **89**, 269–280.
- Starfield, A. M., and F. S. Chapin, 1996: Model of transient changes in Arctic and boreal vegetation in response to climate and land use change. *Ecol. Appl.*, **6**, 842–864.
- Texier, D., and Coauthors, 1997: Quantifying the role of biosphere–atmosphere feedbacks in climate change: Coupled model simulations for 6000 years BP and comparison with paleodata for northern Eurasia and Africa. *Climate Dyn.*, **13**, 865–882.
- Thompson, S. L., and D. Pollard, 1995a: A global climate model (GENESIS) with a land-surface-transfer scheme (LSX). Part I: Present climate simulation. *J. Climate*, **8**, 732–761.
- , and —, 1995b: A global climate model (GENESIS) with a land-surface-transfer scheme (LSX). Part II: CO<sub>2</sub> sensitivity. *J. Climate*, **8**, 1104–1121.
- , and —, 1997: Greenland and Antarctic mass balances for present and doubled atmospheric CO<sub>2</sub> from the GENESIS version 2 global climate model. *J. Climate*, **10**, 871–900.
- UNESCO, 1978: *World Water Balance and Water Resources of the Earth*. UNESCO, 663 pp.
- Wang, W.-C., G.-Y. Shi, and J. T. Kiehl, 1991: Incorporation of the thermal radiative effect of CH<sub>4</sub>, N<sub>2</sub>O, CF<sub>2</sub>Cl<sub>2</sub>, and CFCI<sub>3</sub> into the NCAR Community Climate Model. *J. Geophys. Res.*, **96**, 9097–9103.
- Wetherald, R. T., and S. Manabe, 1995: The mechanisms of summer dryness induced by greenhouse warming. *J. Climate*, **8**, 3096–3108.